inorganics

MDPI

Article

Research on the Hydration and Mechanical Properties of NAC-Hardened Cement under Various Activation Methods

Shiyi Zhang [1,2], Yingfang Fan [1,*] and Surendra P. Shah [3]

[1] Institute of Road and Bridge Engineering, Dalian Maritime University, Dalian 116026, China
[2] School of Civil Engineering and Architecture, Shandong University of Technology, Zibo 255000, China
[3] Civil and Environmental Engineering, Northwestern University, Evanston, IL 60208, USA
* Correspondence: fanyf@dlmu.edu.cn

Abstract: Adding mineral admixture is one of the leading technical ways to improve the durability of cement-based materials. Nano attapulgite clay (NAC) is a unique fiber rod crystal structure that can change the physical and mechanical properties of cement-based materials, and opens up a new idea for exploring the durability of high-performance cement-based materials. This paper studied the effects of NAC on the hydration process, pore structure, and mechanical properties of a cement substrate under different activation methods. The results show that the pH value of the pore solution of cement mixed with 5% NAC high-viscosity ore (calcined) was 8.8% higher than that of the cement without NAC. The chemically bound water contents in the 1% and 3% NAC raw (calcined) cement were 14.11% and 14.04%; when the content of calcined NAC raw ore was 1%, the improvement effect on the cement hydration process is the best. The content of calcined NAC was 1%, 3%, and 5%, and the porosity of hardened cement paste was 19%, 19.04%, and 22.27% lower than that of the cement without NAC. Calcining NAC raw ore can improve cement's hydration process, promote cement's hydration reaction, and increase the compactness of hardened cement paste. The fluidity of the cement mortar mixed with calcined high-viscosity ore (D and E) at a mixing amount of 5% was reduced by 32.66% and 26.13%, respectively, compared to the ordinary specimens. The flexural strength of the cement paste mixed with calcined raw ore and high-viscosity ore at a mixing amount of 1% was generally improved by 28.40% and 17.28% compared to the cement without NAC paste. After calcination, the NAC raw ore is better than the high-clay ore in improving the mechanical properties of cement.

Keywords: NAC; chemical-bound water; porosity; cement hydration; flexural strength; compressive strength

Citation: Zhang, S.; Fan, Y.; Shah, S.P. Research on the Hydration and Mechanical Properties of NAC-Hardened Cement under Various Activation Methods. *Inorganics* **2022**, *10*, 124. https://doi.org/10.3390/inorganics10090124

Academic Editor: Richard Dronskowski

Received: 10 July 2022
Accepted: 22 August 2022
Published: 26 August 2022

1. Introduction

As one of the most popular building materials in the world, cement concrete has been widely used in construction, water conservancy, bridges, roads, and other infrastructure constructions. However, during the service process of reinforced concrete structures, the corrosion of steel bars will be caused by the corrosion of chloride salts, leading to rust expansion and the cracking of concrete. Due to temperature changes, the pore water will freeze–thaw in the cold environment, and multiple freeze–thaw cycles will lead to concrete frost heave cracking [1–4]. The combined action of various complex factors often causes the structure of most buildings to fall far short of their designed service life. To improve the durability of reinforced concrete structures, starting from the material level in order to explore high-durability concrete materials suitable for harsh environments is necessary. At present, adding mineral admixtures is one of the key technical ways to improve the durability of cementitious materials [5,6]. Nano-silicon-dioxide [7–10], nano-calcium-carbonate [11,12], nano-kaolin [13–15], and carbon nanotubes (CNTs) [16] are the major nano-scale admixtures used in cement-based materials. However, despite the unique

advantages of nano-admixtures, it is difficult to prepare nano-silicon-dioxide and CNTs. Furthermore, there are different standards and expensive costs, making their application a problem in practical constructions [17–23].

Studies have shown that nano clay can improve cement-based materials' working performance and durability. As a clay mineral with unique advantages and low prices, nano attapulgite clay provides a new research direction for enhancing the durability of concrete. Attapulgite is a type of magnesium aluminum silicate clay. It has a high specific surface area, high adsorption capacity, is less sensitive to salt, and becomes thixotropic in the presence of electrolytes. These properties make it popular in many industrial applications, such as plastering mortar, precast concrete elements, and oil well drilling mud, especially when high thixotropy is desired [20,24]. Attapulgite also shows good properties for enhancing the new state properties of cementitious materials. Kawashima et al. [25] found that the cement paste's cohesion and adhesive property improved, and the cement paste's shear force resistance was at least 67% higher than that of ordinary specimens after the addition of NAC. Lindgreen et al. [26] explored the impact of NAC on the hydration property of cement mortar. They discovered that NAC could improve the surface property of particles inside the cement paste, with the calcium silicate hydrate (C-S-H) gel growing on the surface of clay particles and the gel nanostructure under the influence of NAC. After NAC was added to account for 11% of the cement in mass, the porosity measured by mortar nitrogen adsorption was nearly 50% higher than that of ordinary specimens. According to all of the test results from the NAC studies [20], the NAC addition in cementitious materials decreases formwork pressure and increases the static and dynamic yield stress. NAC addition also mitigates sand migration in fresh mortars [27].

It has been a concern in the concrete industry that NAC in sand and aggregates adsorb superplasticizers and deteriorate water-reducing agents' efficiency. However, the reinforcement effect of NAC on cementitious materials has great discrete and significant differences, as evidenced by the conflicting research results [22–26]. The research on NAC is mainly limited to improving the workability performance. The research on mechanical properties and durability is not enough, and the research on the microstructure and composition effect of cement-based materials is insufficient.

In this paper, the effects of various activation methods of nano attapulgite clay on the physical and mechanical properties and durability of cement-based materials are investigated. SEM and XRD analysis was carried out to detect the effect of calcination on the microstructure and mineral phase of NAC. The influence of calcined NAC on the hydration reaction and pore structure of cement was analyzed. The content of chemically bound water, pH value of the pore solution, and porosity of cement were measured. The effect of calcined NAC on the relationship between the compressive strength of cement paste and the chemical-bound water content was established.

2. Materials and Methods

2.1. Raw Materials

Materials

The raw ore and high-viscosity ore produced by Changzhou Dingbang Mineral Products Technology Co., Ltd. (Changzhou, China), with ore sourced from Xuyi County of Jiangsu Province, were used as the NAC in the experiment; the chemical composition of the NAC is presented in Table 1. The octadecyl trimethyl ammonium chloride produced by Shandong Banghua Oil Chemistry Co., Ltd. (Weifang, China) was adopted as the cationic surfactant; the physical properties are presented in Table 2. A concentrated hydrochloric acid with a concentration of 12 mol/L was used.

Table 1. Composition of NAC.

Component	CaO	SiO_2	Al_2O_3	Fe_2O_3	MgO	K_2O	Na_2O	Lol
Content/%	1.8–2.5	50.4–61.3	9.4–9.5	4.0–5.0	9.3–10.5	0.2–0.6	0.5–1	11.94–13.46

Table 2. Physicalindex of stearyl trimethyl ammonium chloride.

Appearance (25 °C)	Active Substance Content (%)	Free Amine Content (%)	pH (1% Aqueous Solution, 25 °C)
White waxy particles	≥90	≤1.0	6.0–8.0

2.2. Preparation of Specimens

Raw ore (A) and high-viscosity ore (B) were selected as the raw materials, with the chemical activity improved by regulating the calcination temperature. The raw ore and high-viscosity ore that had been calcined at a temperature of 650 °C for 2 h were marked as C and D, respectively, whereas the high-viscosity ore that had been calcined at a temperature of 750 °C for 2 h was marked as E. The raw ore that had undergone hydrochloric acid modification was marked as A-H, whereas the raw ore that had been modified through surface bioactive treatment was marked as A-O. Ultrasonic dispersion was applied to the foresaid five types of NAC (A, B, C, D, and E), which were subsequently marked as A-C, B-C, C-C, D-C, and E-C, respectively. The sample numbers are shown in Figure 1.

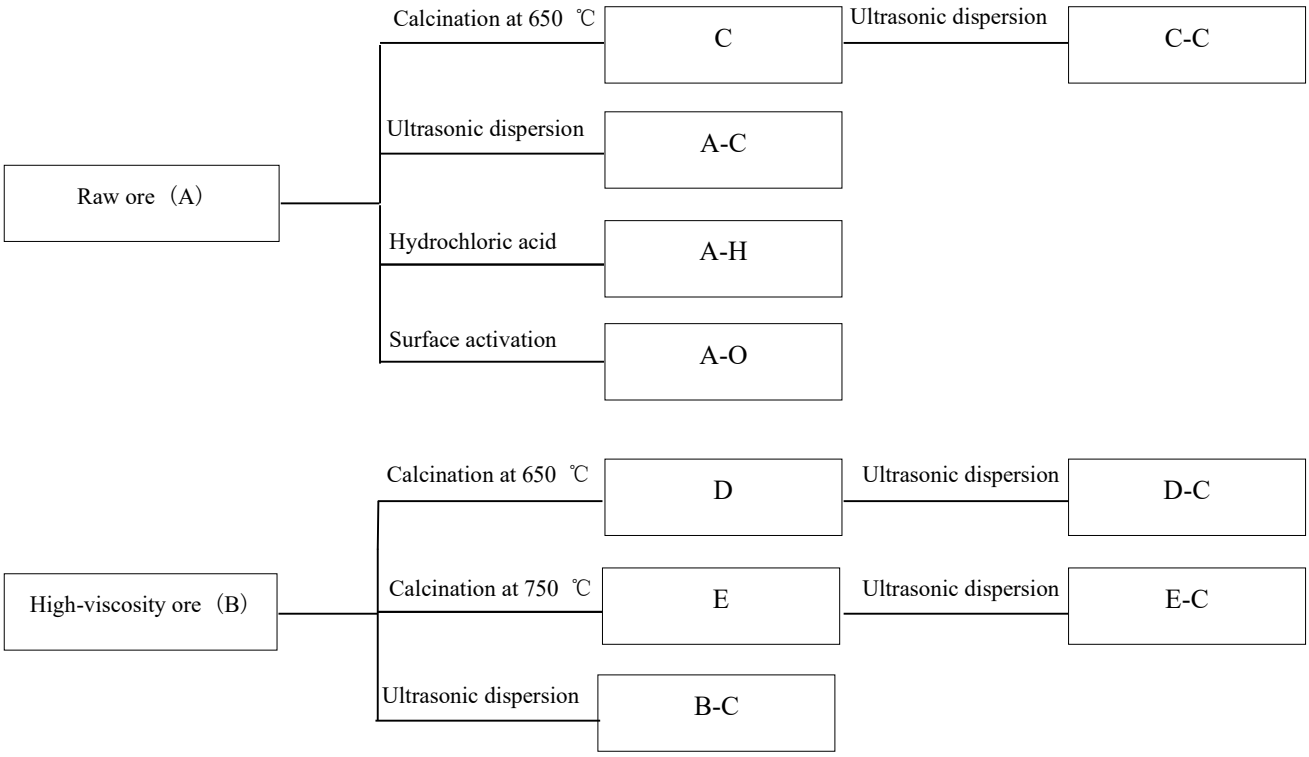

Figure 1. Different activation methods and sample numbers of NAC.

To study the effect of NAC on cement hydration, pore structure, and mechanical properties, four NAC were selected in this paper, namely raw ore (A), high-viscosity ore (B), calcined raw ore (C), and calcined high-viscosity ore (D). The cement specimen had a water–binder ratio of 0.5 and the content of NAC accounted for 0%, 1%, 3%, and 5% of the total mass of the cementitious material, respectively. When preparing the specimens, refer to the cement paste mixing method in "Highway Engineering Cement and Cement Concrete Test Regulations" (JTG E30-2005).The mixing proportion of cement paste with NAC is shown in Table 3.

Table 3. Mixing proportion of cement paste with NAC (raw ore and high-viscosity ore) under different activation methods.

Specimen Number	Cement/%	NAC/%
CS	100	0
A1 [1], B1, C1, D1	99	1
A3, B2, C3, D3	97	3
A5, B5, C5, D5	95	5

[1] Sample No. A1 refers to the sample of NAC raw ore, and the mixing addition is 1% of the total mass of cementitious material.

2.3. Test Methods and Processes

2.3.1. High-Temperature Calcination

A SX2-8-10 chamber electric furnace was used for high-temperature calcination. Prior to this, the sampled powder was sealed into a crucible that was placed in the furnace for calcination. The crucible was fetched out for cooling and further processing only after the temperature had risen to the specified temperature and had been sustained for 2 h.

2.3.2. Hydrochloric Acid Acidification

After being diluted with distilled water to a concentration of 6 mol/L, the hydrochloric acid was mixed with the raw ore at a solid-to-liquid ratio of 2:3. The mixed solution was stirred evenly and left to stand for acidification for 24 h. Then, distilled water was used for washing until the supernatant liquid turned neutral without chloride ions (a 0.01-mol/L silver nitrate solution for detection). The solution was subsequently dried in an evaporating dish to form the test specimen A-H.

2.3.3. Surface Activation

According to the reference [28], the raw ore was placed into the distilled water to form a turbid liquid. Then, the temperature was raised to 80 °C with a water bath, after which, octadecyl trimethyl ammonium chloride, weighed at 2% of the raw ore in mass, was added as the surfactant. The solution was cooled to room temperature after stirring and activation under the same temperature for 3 h. Then, it was dried in an evaporating dish to form the test specimen A-O.

2.3.4. Ultrasonic Oscillation

A turbid liquid of NAC prepared at a certain proportion was placed in a DS-5510DTH ultrasonic cleaner. Then, ultrasonic waves higher than 20 KHz were released to disperse the turbid liquid for 15 min. The turbid liquid obtained was used for dispersibility evaluation directly.

2.3.5. Dispersibility Evaluation

According to the reference [29], the sedimentation method was used as the dispersibility evaluation standard in this section. Most of the systems with poor dispersion stability presented agglomerate flocculating sedimentation, with the formation of a clear interface between the sediments and the supernatant liquid, and a sedimentation equilibrium within a short time. The systems with superior dispersion stability displayed a slow sedimentation rate and a dispersed distribution of particles that gradually thickened from the top to the bottom. No obvious sediments were spotted in such systems. Specific steps in the test are as follows: the dispersed systems were poured into a measuring cylinder, left to stand, and subsequently monitored for changes in the sediment volumes over time. Meanwhile, the turbid liquid was placed in a colorimetric tube for direct observation of the dispersion properties of different dispersion methods.

2.3.6. Composition Analysis and Microscopic Observation

A composition analysis of the specimens was conducted via a D/MAX-Ultima XRD. A SUPRA 55 SAPHIRE field emission scanning electron microscope (FESEM) was used for electron microscopic scanning of the microstructures of the specimens [30,31].

2.3.7. Chemically Bound Water Content

After the specimens were maintained to the specified age, they were immediately ground and passed through a 0.08 mm square-hole sieve. Onegram of powder (accurate to 0.0001 g) was weighed on an analytical balance, put into a ceramic crucible with a lid, and dried in an oven at 65 °C for 24 h, and the mass m1 was weighed after drying. Then, the crucible was moved to the muffle furnace and calcinated at a temperature of 1050 °C for 2 h, and the mass m_2 was considered. The chemically bound water content in the cement slurry was calculated according to Formula (1).

$$\begin{cases} w = \frac{\frac{m_1 - m_2}{m_1} - L}{1 - L} \times 100\% \\ L = (1 - \alpha)L_c + \alpha L_a \end{cases} \quad (1)$$

In the formula, w is the chemically bound water content, %; m_1 is the mass of the sample after drying, g; m_2 is the mass of the sample after calcination, g; α is the content of nano attapulgite clay, %; L_c is the cement calcination loss, %, L_a is the loss on ignition of nano attapulgite clay, %.

2.3.8. Well Solution pH

When the specimens were maintained to the specified age, they were immediately taken out, ground, and passed through a 0.08 mm square-hole sieve. Three grams of powder (accurate to 0.0001 g) was weighed into a beaker with an analytical balance, 30 mL of distilled water was added in order to disperse for 15 min ultrasonically, and then the result was left to stand for 12 h. The pH value of the supernatant test solution was taken as the alkalinity value of the cement slurry pore solution.

2.3.9. Pore Content and Microstructure

The stomatal content was obtained indirectly through the water loss rate of the saturated specimen under specific conditions, that is, the 'evaporable water content method'. After the sample was cured to the specified age, the vacuum saturation was completed according to the American Society for Testing and Materials (ASTM) regulations, and the volume v and mass m of the specimen were measured. Then, it was moved to the standard curing environment, and, after waiting until the mass of the sample tended to remain unchanged, calculate the porosity p of the sample was calculated according to Formula (2).

$$p = \frac{m - m_1}{\rho v} \times 100\% \quad (2)$$

In the formula, p is the pore content, %; m is the mass of the specimen after vacuum water retention, g; m_1 is the mass of the specimen after dehydration, g; v is the volume of the specimen, cm^3; ρ is the density of water, g/mL.

2.3.10. Mechanical Properties

The flexural and compressive strength was tested with reference to the test methods in "Highway Engineering Cement and Cement Concrete Test Regulations" (JTG E30-2005). The flexural test was carried out on a cement electric flexural testing machine with a loading rate of 50 N/s. The compressive strength was tested by a 200 t hydraulic servo pressure testing machine with a loading rate of 0.5 MPa/s.

3. Results and Discussion

3.1. Impacts of Calcination on Composition and Crystal Structures of NAC

Subsubsection

For the four types of water contained in NAC, the research [32] revealed that when the calcination temperature was higher than 400 °C, the adsorption of crystals improved, thereby resulting in the complete dehydration of the adsorbed water and the zeolite water in them. When the temperature rose to 650 °C, the binding water and structural water were removed to generate a large number of active oxides, which indicated a high pozzolanic activity. After calcination at 650 °C, the appearance changes in raw ore and high viscosity is shown in Figure 2. Before calcination, both the original nano attapulgite ore and the high-viscosity ore were gray-white. After calcination at 650 °C, part of the ferrous iron in the clay gradually formed ferric iron, which eventually led to the color of the two nano-clay minerals becoming pale yellow.

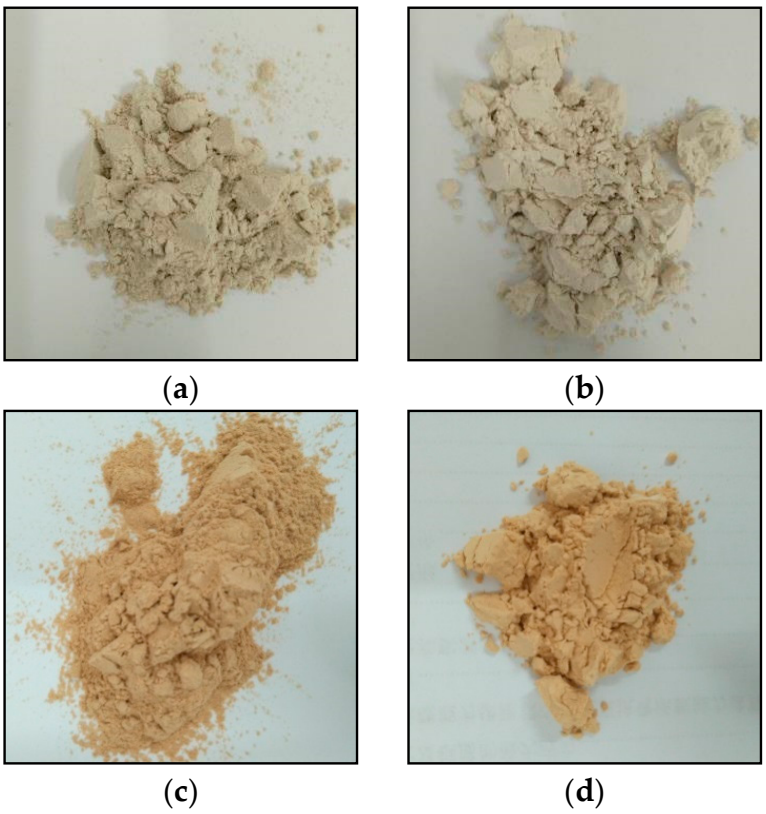

Figure 2. Appearance changes in raw ore and high-viscosity ore after calcination at 650 °C. (**a**) Raw ore; (**b**) High viscosity ore; (**c**) Calcined raw ore under 650 °C; (**d**) Calcined high viscosity ore under 650 °C.

Figure 3 represents the SEM photos of the NAC before and after calcination, revealing a microscopic disordered fibrous structure of the NAC. The fibrous rod-like crystals were approximately tens of nanometers in diameter and 0.5 to 1 μm in length. In addition, it can also be observed that high-viscosity ore rod-like crystals were significantly smaller than raw ore rod-like crystals in both length and diameter, thus leading to a larger specific surface area, adsorbability, and colloidality of the high-viscosity ore when compared to the raw ore. After calcination at 650 °C or 750 °C for 2 h, the structures of NAC crystals underwent no collapse as their fibrous structures remained intact. Since the rod clusters of NAC were opened after calcination, the phenomenon of fibrillar aggregation was significantly reduced.

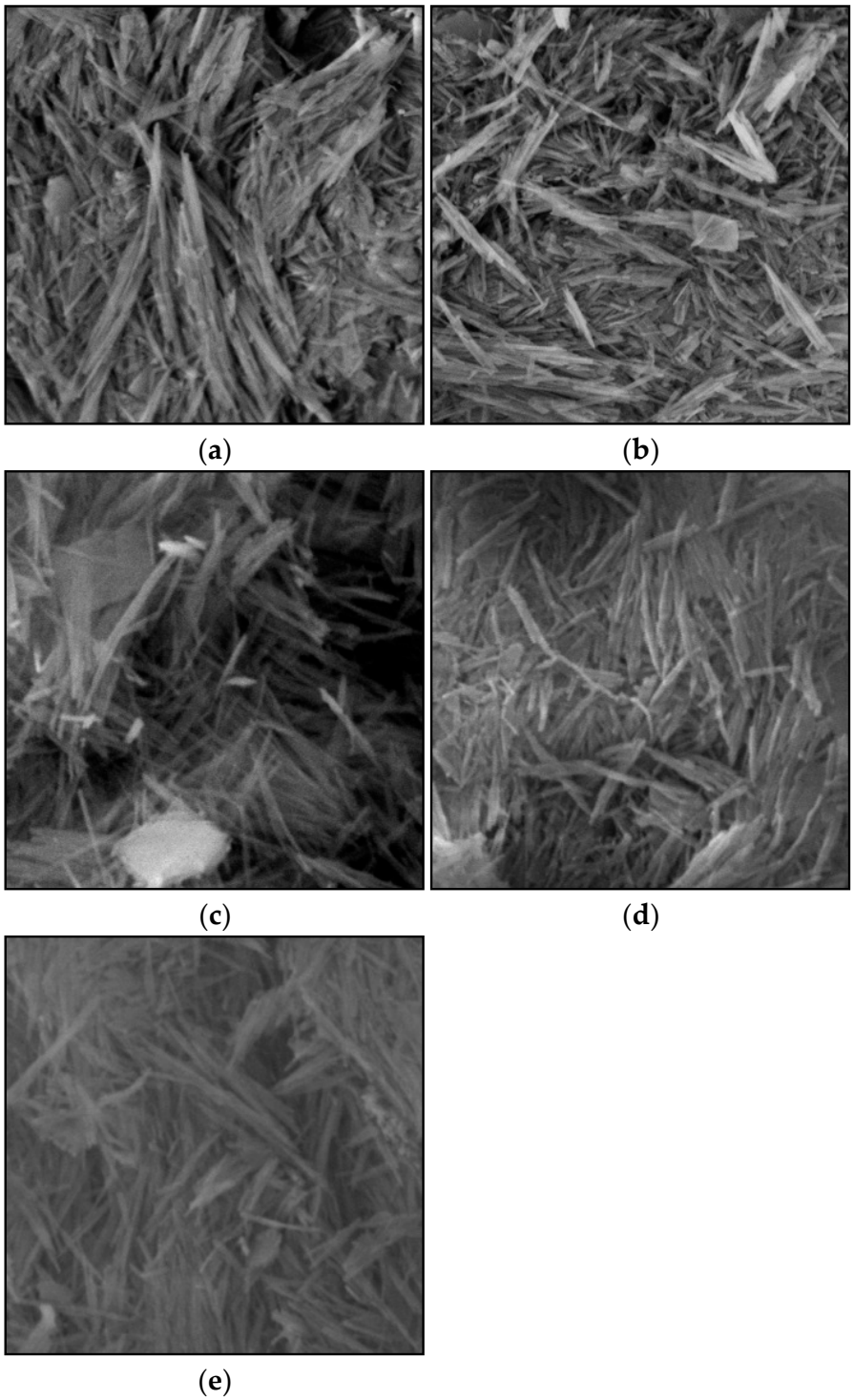

Figure 3. Micrographs of NAC by FESEM (1:10,000). (**a**) Raw ore; (**b**) High viscosity ore; (**c**) Calcined raw ore under 650 °C; (**d**) Calcined high viscosity ore under 650 °C; (**e**). Calcined high viscosity ore under 750 °C.

Figure 4 presents the XRD graphs of the NAC before and after calcination, from which, it can be seen that the diffraction peaks of the NAC disappeared after calcination and a large amount of SiO_2 and alkali metal salt was generated. The NAC was extremely unstable in crystallinity and possessed a high pozzolanic activity.

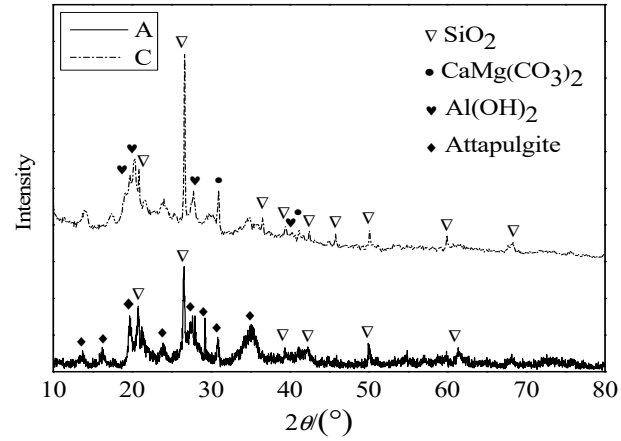

(**a**)

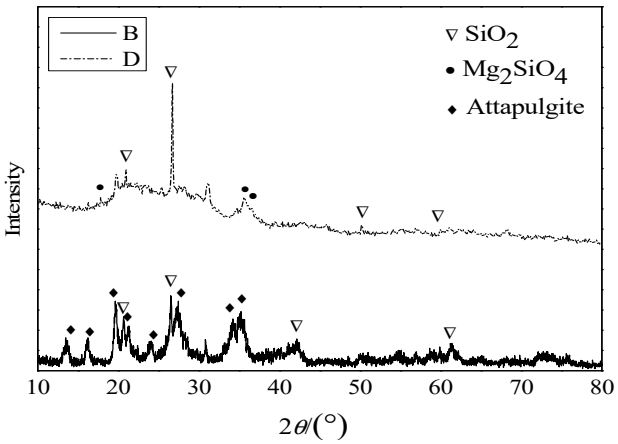

(**b**)

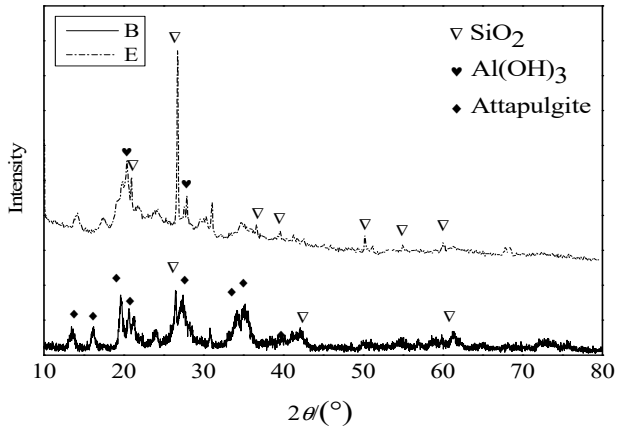

(**c**)

Figure 4. Phase changes in NAC before and after calcination. (**a**) Row ore under 650 °C calcined; (**b**) High-viscosity ore under 650 °C calcined; (**c**) High-viscosity ore under 750 °C calcined.

3.2. Analysis of NAC Dispersibility in Water

The sediment volume fraction of the NAC turbid liquid is shown in Figure 5, from which, it can be seen that the sediment volume enlarged as the mixing amount increased. When the mixing amount was maintained at 1%, the raw ore and the acidified raw ore indicated the worst dispersibility, whereas the raw ore and the high-viscosity ore processed

with ultrasonic dispersion had the best dispersion effect, with those activated and calcinated standing between them. When the mixing amount was at 2%, the acidified raw ore experienced an improvement in dispersibility. When the mixing amount reached 3%, the sedimentation rate of the raw ore decreased to some degree. When the mixing amount rose to 5%, the acidified raw ore indicated the fastest sedimentation rate. To sum up, ultrasonic dispersion improved the dispersion property of NAC, and no sedimentation happened in a short time when the raw ore and high-viscosity ore accounted for 2% of the cement. However, acidification and activation showed no significant impact on the improvement in the dispersibility of raw ore in water.

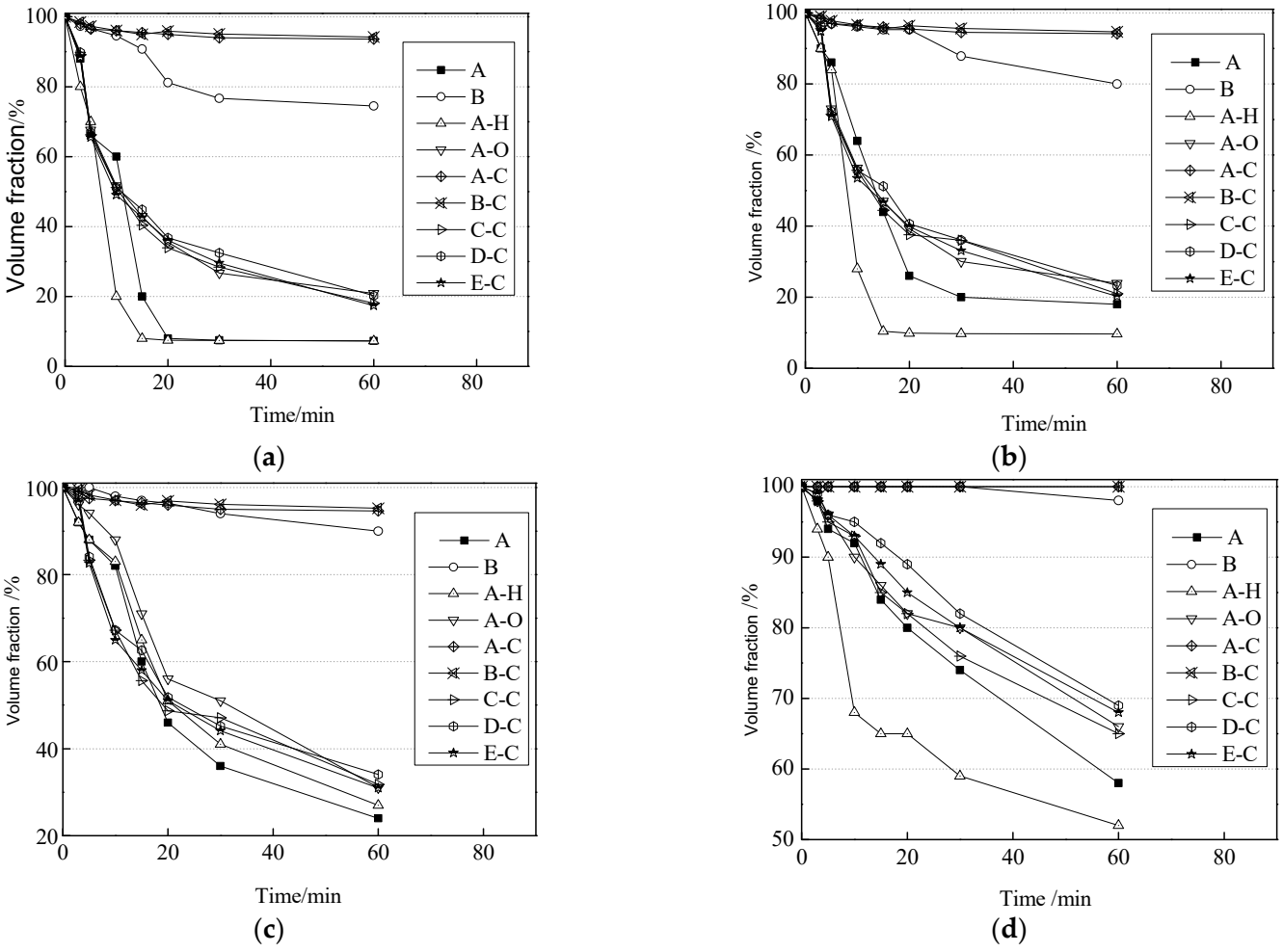

Figure 5. Relationship between settlement volume and time. (**a**) NAC addition: 1%; (**b**) NAC addition: 2%; (**c**) NAC addition: 3%; (**d**) NAC addition: 5%.

The turbid liquid of dispersed NAC was poured into a 25 mL colorimetric tube (shown in Figure 6). Figure 6 reveals that, when the mixing amount was at 1%, the acidified raw ore showed a slightly better effect than those unmodified. Although activated and calcined raw ores were inferior to acidified raw ore in dispersibility, they were much inferior to the raw ore and high-viscosity ore processed via ultrasonic dispersion. It is worth noting that adsorption aggregation is highly common in high-viscosity ore because of its high adsorbability. Therefore, when they agglomerated into floccules, the sediment volume was comparatively lowered.

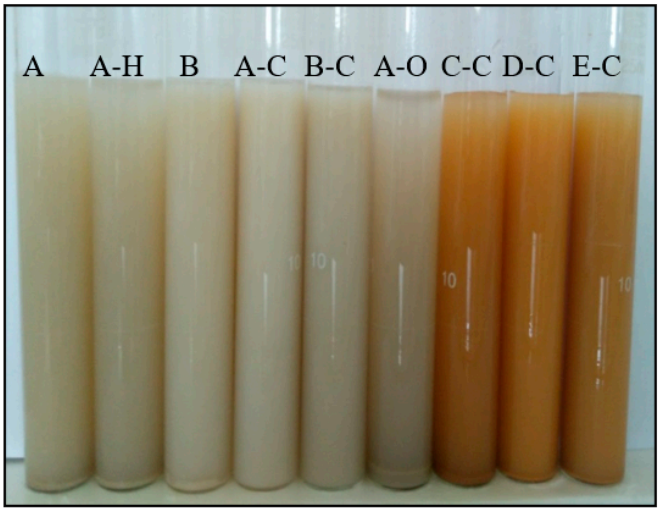

(**a**)

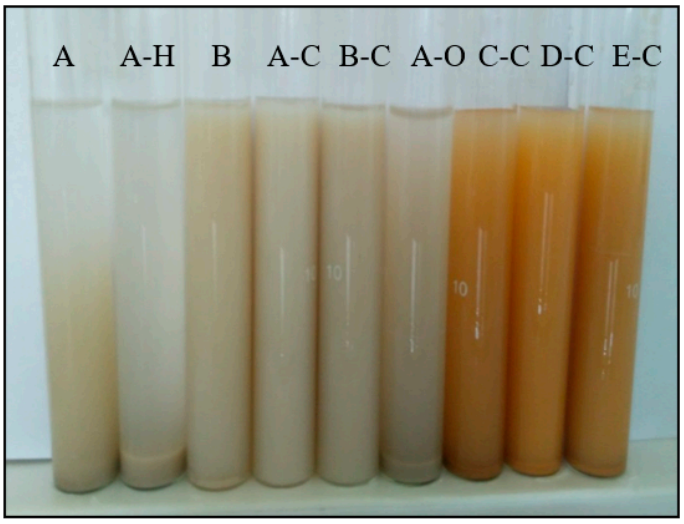

(**b**)

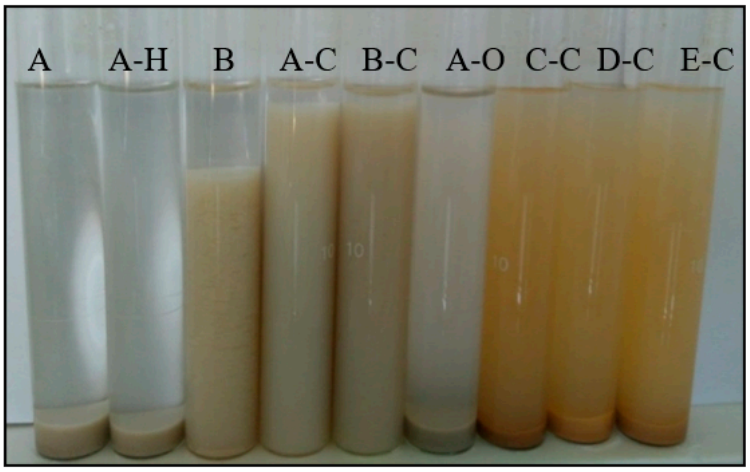

(**c**)

Figure 6. Settlement diagram of NAC (content of 1%). (**a**) 0 min; (**b**) 10 min; (**c**) 60 min.

3.3. Hydration Process of NAC Cement Paste

3.3.1. Analysis of Microstructures

The microstructure of the cement with NAC under 650 °C calcinationis shown in Figure 7. According to Figure 7, the cement paste mixed with calcined NAC had a significantly higher compactness than pure cement paste, while pure cement paste showed larger gel pores as well as a less tight (weaker) bond between its hydration products. Figure 7 also reveals fibrous rods in the cement paste mixed with NAC, which had no bifurcations at the ends. Therefore, the impact of C-S-H gels was deemed insignificant. The early-strength Portland cement used in this test has a high C3A content, and NAC has a high aluminum content as well; as such, the two elements combined to cause a reduced stability in ettringites. Due to drying at a temperature of 75 °C for 24 h before electron microscopic scanning, most of the ettringites would have been decomposed by the heat if there were any. Moreover, the fluidity of the cement paste mixed with uncalcined NAC was not improved, thus indicating a poor performance of uncalcined NAC when integrating with the cement paste. Since no significant bunched ettringite crystals were observed in the cement paste, it was inferred that this kind of fibrous rod was NAC. It can be seen that the fibrous rods in b and c were significantly more compact than those in d and e. This was because the low activity of uncalcined NAC would prevent it from participating in the hydration process. Based on Figure 7, the cement paste mixed with uncalcined NAC contained a large amount of flocculent hydrated silicate gels after 28 d. The paste structure was relatively loose and not compact enough, showing numerous gel pores. However, the hydrated silicate gel mixed with calcined NAC had a compact structure with rod-like crystals tightly bonded with surrounding hydration products, thus indicating the significantly improved compactness of the paste.

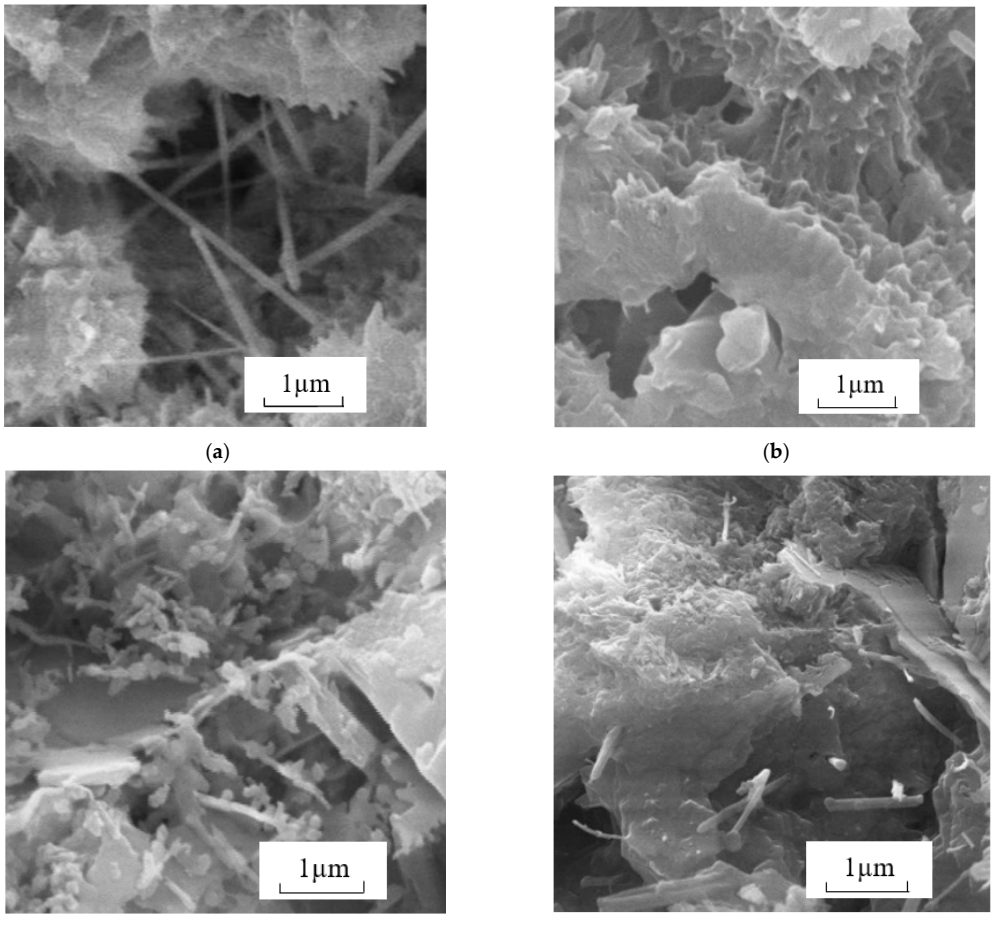

(**a**) (**b**)

(**c**) (**d**)

Figure 7. *Cont.*

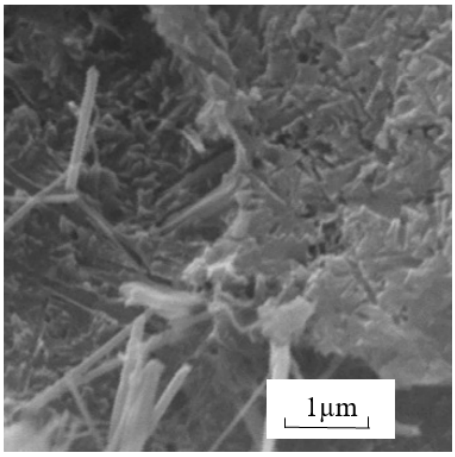

(**e**)

Figure 7. Microstructural changes of the cement with raw ore and high-viscosity ore under 650 °C calcination. (**a**) CS; (**b**) A5; (**c**) B5; (**d**) C5; (**e**) D5.

3.3.2. Chemical Immobilized Water Content

The chemical immobilized water content was tested when the test specimens were maintained at corresponding ages. The test results are shown in Figure 8. It can be seen that the chemically bound water content of the cement slurry increased rapidly in the early stage. Still, after 7 days of age, the growth trend of the chemically bound water content of each sample gradually slowed down, and the growth rate decreased. From Figure 8a,b at 3 days of age, we can obtain that the chemically bound water content in the cement with different ranges of the NAC raw ore (uncalcined) was 11.06%, 11.06%, 10.81%, and 10.97%. The chemically bound water content in cement mixed with high-viscosity ore (uncalcined) was 11.05%, 10.78%, 10.15%, and 10.69%. With the increase in the content, the uncalcined NAC reduces the hydration process of the cement. The chemically bound water content in the raw ore cement with the addition of 3% NAC is 12.78% at 28 days, and the chemical-bound water content in the high-viscosity ore cement is 13.31%, which indicates that the long-term activity of the raw ore is higher than that of the clay ore. From Figure 8c,d, it can be drawn that the movement of the calcined NAC has been improved. The chemically bound water contents in the 1% and 3% NAC raw (calcined) cement were 14.11% and 14.04%, which were higher than those in the NAC high-viscosity ore cement (13.96% and 13.58%). When the content of calcined NAC raw ore is 1%, the improvement effect on the cement hydration process is the best.

From the above, it can be concluded that a small amount of calcined NAC helped to increase the chemical-immobilized water content of the cement paste, and this can be attributed to the sharply increased activity of calcined NAC. As the mixing amount increased, the total hygroscopicity of NAC is expected to rise as well, leading to a reduced water–binder ratio in the vicinity of cement particles. A comparison between c and d of Figure 8 reveals that the hydration process of the cement paste accelerated at a later stage because of the water retention effect of calcined high-viscosity ore, thus causing its overall hydration degree to stay at basically the same level as that of the cement paste mixed with calcined raw ore.

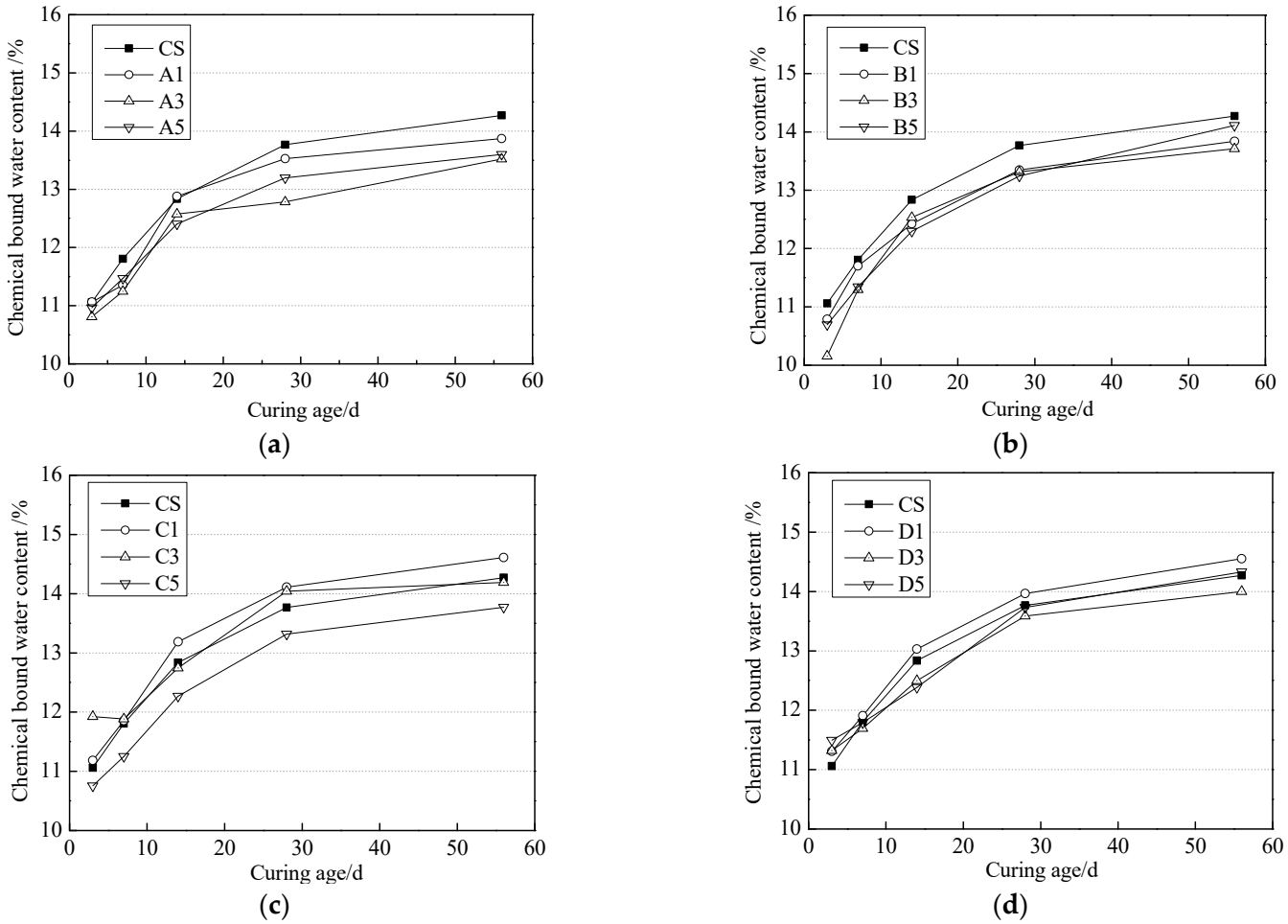

Figure 8. Chemical-binding water content of cement with NAC under 650 °C calcination. (**a**) Raw ore; (**b**) High-viscosity ore; (**c**) Raw ore under 650 °C calcined; (**d**) High-viscosity ore under 650 °C calcined.

3.3.3. The pH Value of Pore Solutions

When curing the specimens to the corresponding ages, the pH values of their pore solutions were tested by the stripping method, as shown in Figure 9. It can be seen that the pH value of pure cement paste pore solutions increased quickly in the early stage because the hydration reaction rate became fast due to the sufficient water around the cement particles. Massive sulfate ions were also consumed, thereby releasing a notable amount of hydroxyl ions to maintain the charge balance. Simultaneously, the solidified alkali metal ions were also released, causing the pH value of the pore solutions to rise continuously. As hydration deepened, the reaction rate tended to be gentle and the hydroxyl ion concentration was basically balanced, thereby causing the pH value of the pore solutions to lean towards remaining unchanged. The pore solutions of the cement paste mixed with uncalcined NAC showed a generally lower pH value than that of pure cement paste, with the value being lowest when the mixing amount reached 5%. The pH value of the cement paste pore solutions could be enhanced by adding calcined NAC, with a mixing amount between 1% and 5%.

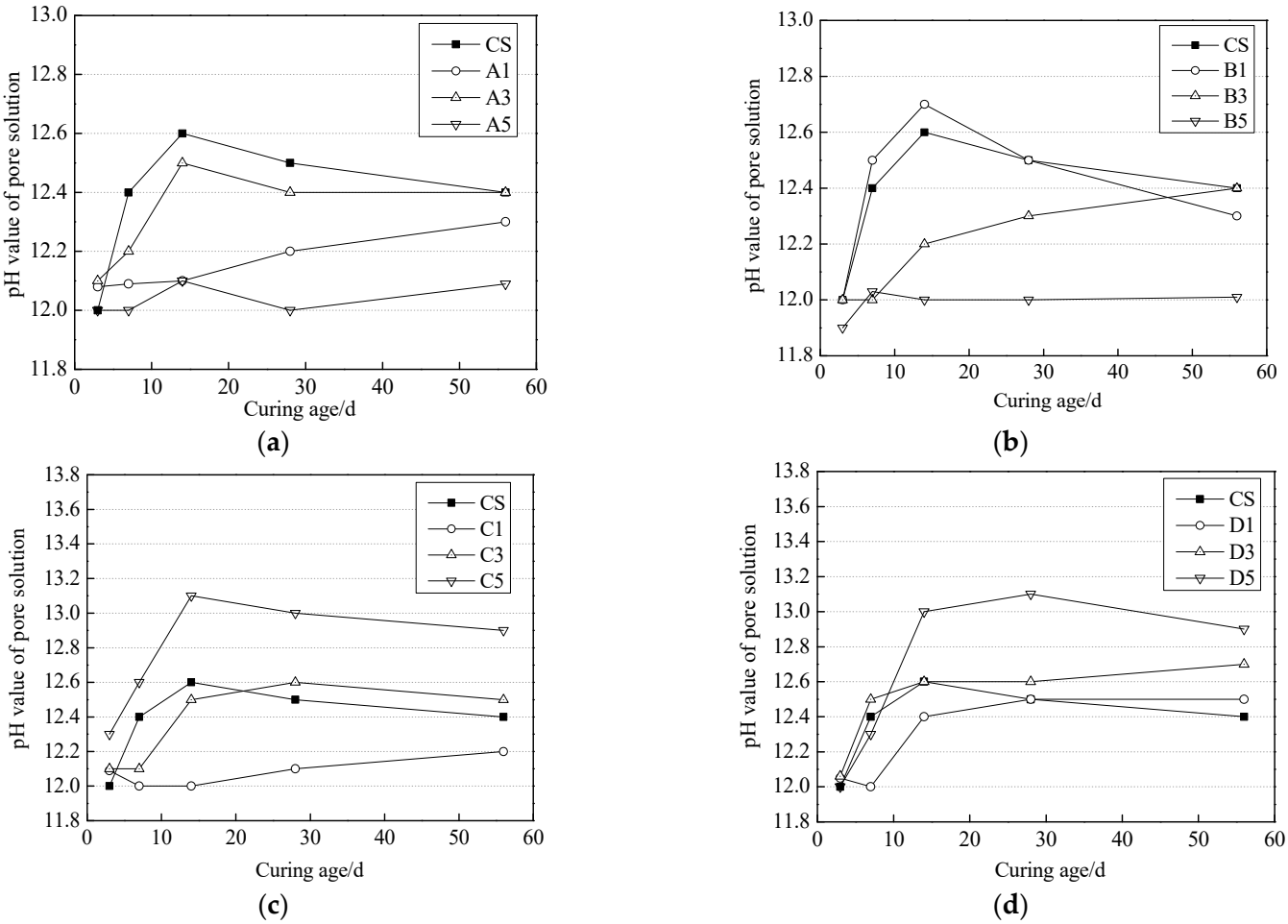

Figure 9. pH value of pore solution in cement paste with NAC after 650 °C calcination. (**a**) Raw ore; (**b**) High-viscosity ore; (**c**) Raw ore under 650 °C calcined; (**d**) High-viscosity ore under 650 °C calcined.

From Figure 9a,b, it can be seen that the pH value of the pore solution of the cement slurry mixed with uncalcined NAC is generally lower than that of the cement slurry without NAC, and both are the lowest when the dosage is 5%. When the curing age is 14 days, the pH value of the pore solution of the cement mixed with the NAC raw ore is 3.96%, 3.95%, and 0.1% lower than that of the cement without NAC, indicating that the 5% NAC raw ore cement has a sufficient hydration reaction. The pH value of the pore solution of NAC high-viscosity mineral cement with a dosage of 1% is 12.7, which is higher than the pH value of cement without NAC (12.6), indicating that the hydration activity of cement mixed with 1% high-viscosity mineral is high. In Figure 9c,d, it can be seen that the pH value of the solution in the cement mixed with 5% NAC (calcined) is higher than that of the cement without NAC. When the curing age is 14 days, the pH value of the mesoporous solution of the NAC raw ore(calcined) cement is 3.96% higher than that of the cement without NAC. The pH value of the mesoporous solution of the NAC high-viscosity ore (calcined) cement is 8.8% higher than that of the cement without NAC.

3.4. Fluidityof the Cement Paste Mixed with NAC

The fluidity of the cement mortar was measured immediately after it had been mixed, and the results are shown in Figure 10. It is observed that the fluidity of the cement mortar mixed with NAC decreased with the increase in the mixing amount. When the mixing amount of uncalcined raw ore and high-viscosity ore was at 5%, the fluidity of the cement mortar was reduced by 45.23% and 57.27%, respectively. This is in comparison to the fluidity of the ordinary specimens. Hence, the fluidity is greatly reduced, which

will, in turn, seriously affect the workability of the cement-based materials. This can be explained by two reasons. Firstly, owing to the strong hygroscopicity and colloidality of the NAC, the original water in the cement void was adsorbed by the pores of the NAC rod-like crystals, which then decreased the water–binder ratio and made the mortar viscous, particularly for its colloidality. Secondly, the microstructures of the NAC possessed a great amount of chaotic fibrous rod-like crystal structures, which aggregated into a mass in an extremely easy manner. When they were mixed with the cement mortar, the internal friction resistance was increased so as to decrease fluidity. The figure also reveals that, for the high-viscosity ore specimen after ultrasonic dispersion, the fluidity of its cement mortar was relatively lower than that of the high-viscosity ore without ultrasonic dispersion. This was mainly because the fibrous rod-like crystal mass of the NAC was unfolded by the ultrasonic dispersion and its specific surface area was enlarged. Therefore, the fibers were increased, and both the hygroscopicity and internal friction resistance were strengthened, thus reducing the fluidity of the cement mortar. It can also be seen in the figure that the fluidity of the cement mortar mixed with calcined NAC was prominently greater than that of the cement mortar mixed with uncalcined NAC. In addition, the fluidity was enhanced with the increase in calcination temperature, as derived by the fact that the fluidity of the cement mortar mixed with calcined high-viscosity ore (namely D and E) at a mixing amount of 5% was reduced by 32.66% and 26.13%, respectively, in comparison to the ordinary specimens. The major cause was that the decrease in colloidality of calcined NAC was much larger than the increase in its adsorbability. Consequently, parts of the rod-like crystals were broken and collapsed, the seamed edges became sleeker, and the internal friction resistance was smaller than that of uncalcined NAC.

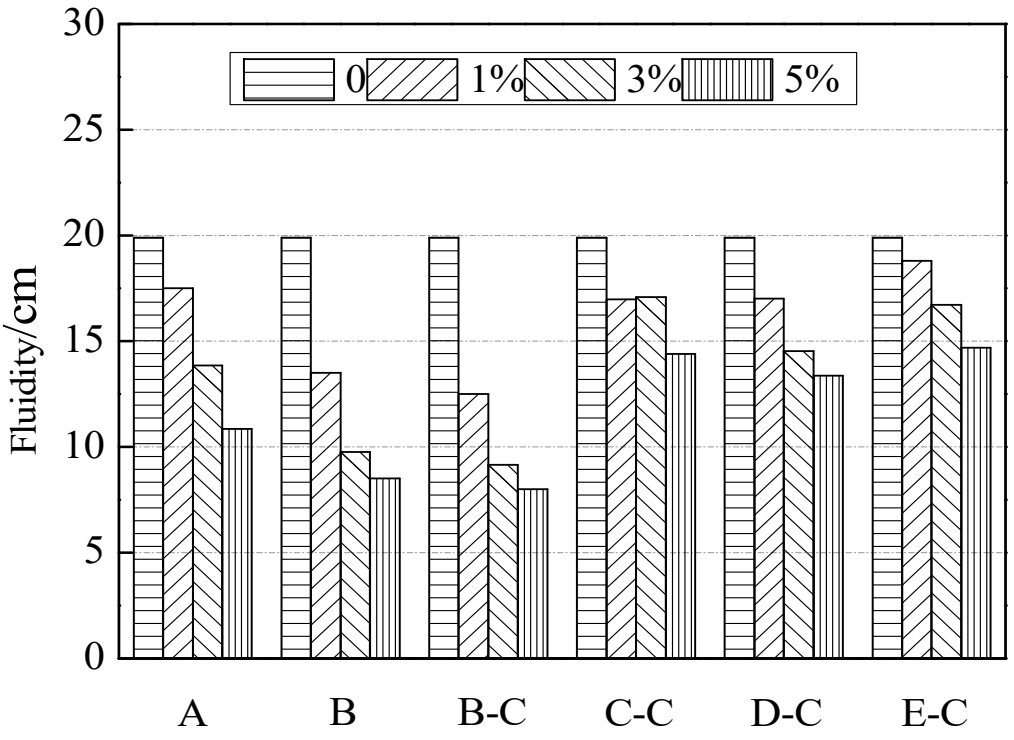

Figure 10. Fluidity of cement mortar with various NAC addition.

3.5. Mechanical Properties of the Cement Paste Mixed with NAC

3.5.1. Flexural Strength

The flexural strength and pore content were tested as the specimens were cured to an age of 28 d, and the results are displayed in Figure 11.

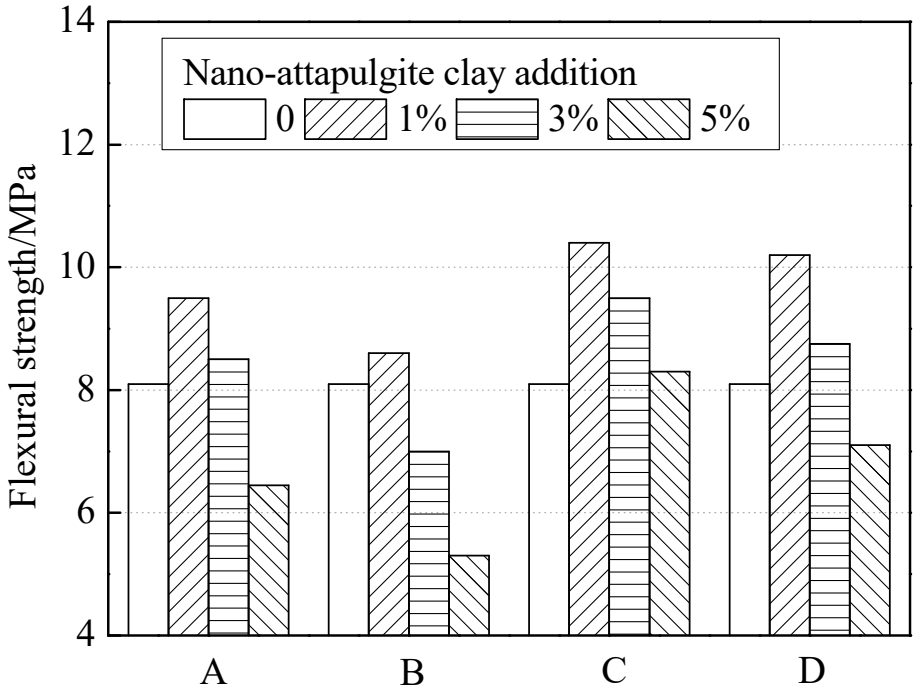

Figure 11. Flexural strength of cement paste with various NAC addition.

It can be found in Figure 11 that the four types of NAC possessed the greatest flexural strength at a mixing amount of 1%, and that the flexural strength gradually declined as the mixing amount increased. The flexural strength of the cement paste mixed with calcined raw ore and high-viscosity ore at a mixing amount of 1% was generally improved by 28.40% and 17.28%, respectively, when compared to that of the cement without NAC. It was discovered in the test that the addition of a small amount of uncalcined NAC could improve the workability of the cement paste. However, with the increase in the mixing amount, the fluidity of the paste was increasingly poorer. As such, it was difficult for the paste to vibrate and compact, resulting in the introduction of a large number of pores, which were most obvious in the high-viscosity ore. As a natural mineral, uncalcined NAC is characterized by a relatively stable chemical property. Therefore, when it was added into the cement paste, it existed as an impurity such that hydration could hardly be activated. The activity of the calcined NAC was also raised substantially. Moreover, the colloidality of the NAC was reduced through high-temperature calcination, thereby decreasing the influence on the workability of the cement paste.

3.5.2. Compressive Strength

The compressive strength test was carried out when the specimens were cured to an age of 28 d, and the results are shown in Figure 12. It reveals that the compressive strength of the cement paste was reduced by the addition of uncalcined NAC, and the decrease in the compressive strength of the cement paste mixed with high-viscosity ore was especially significant as the mixing amount increased. The compressive strength of calcined raw ore cement with a 1%, 3%, and 5% content is 6.5%, 2.29%, and 7.25% lower than that of the cement without NAC; the strength of calcined high-clay cement with a 1%, 3%, and 5% content is 4.11%, 9.25%, and 2.31% lower than that of the cement without NAC. This was because, on the one hand, uncalcined NAC's comparatively significant impact on the cement paste's fluidity lowered the matrix's compactness. On the other hand, uncalcined NAC existed in the cement paste as an impurity because its low activity made it difficult for it to participate in the hydration. Consequently, the compressive strength of the cement paste mixed with calcined NAC was remarkably improved as the mixing amount increased. In the test, the compressive strength of calcined raw ore cement with a 1%, 3%, and 5%

content is 4.5%, 8.06%, and 9.38% higher than that of the cement without NAC; the strength of calcined NAC high-clay cement with a 1%, 3%, and 5% content is 1.84%, 2.76%, and 2.86% higher than that of the cement without NAC.

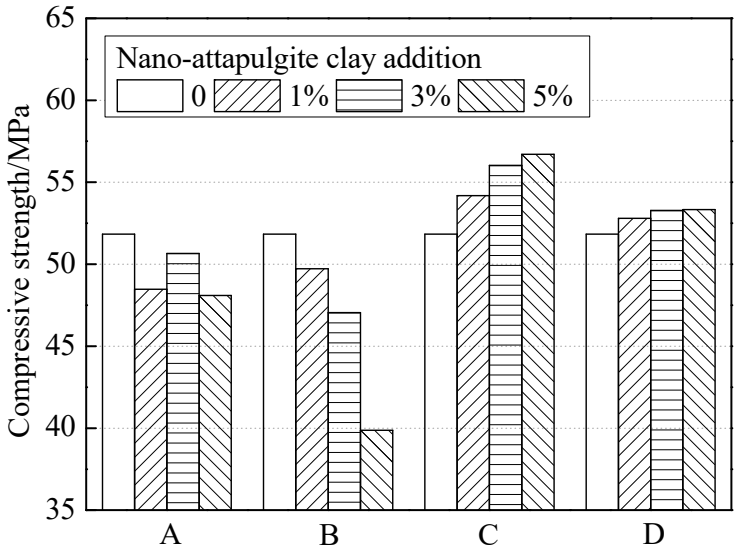

Figure 12. Compressive strength of cement paste with various NAC addition.

The chemical-binding water content of cement paste with various NAC addition is shown in Figure 13. From Figure 13, we can draw that the addition of uncalcined NAC decreased the chemical immobilized water content of the paste, thereby presenting a low degree of hydration. In addition, because of its strong hygroscopicity, uncalcined NAC adsorbed plenty of free water into its fibrous rod-like crystals and reduced the water–binder ratio around the cement particles. Adding calcined NAC can improve the hydration degree of slurry. When adding 1% and 3% calcined NAC raw ore, the chemical-bound water content of cement is 2.5% and 1.99% higher than cement without NAC. The chemical and chemical-bound water content of the cement with 1% NAC is 1.43% higher than that of cement without NAC. This is mainly because calcined NAC's colloidal and adsorption properties are reduced, but the chemical activity is significantly enhanced. It no longer exists in the slurry as impurities but directly participates in the hydration process.

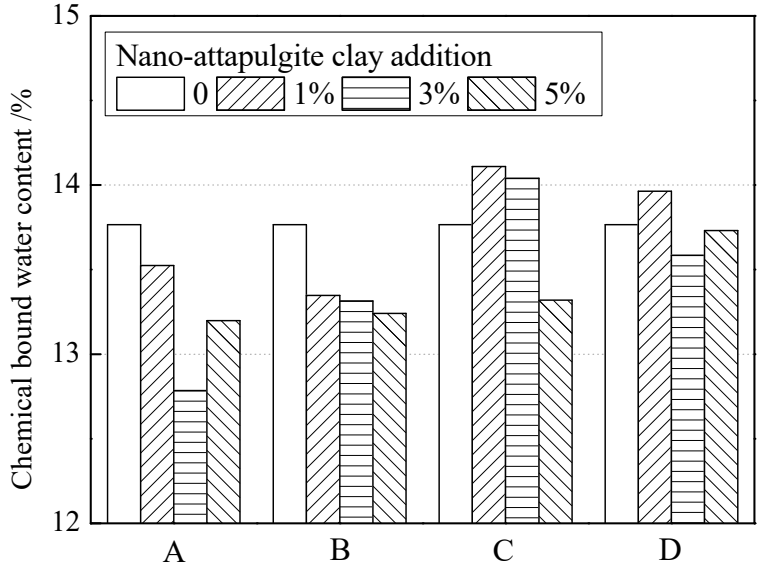

Figure 13. Chemical-binding water content of cement paste with various NAC addition.

Figure 14 shows the relationship between the compressive strength of the cement paste and the chemically immobilized water content, which was positively correlated. This indicated that the addition of calcined NAC could raise the hydration degree of the cement paste, thus improving its compressive strength.

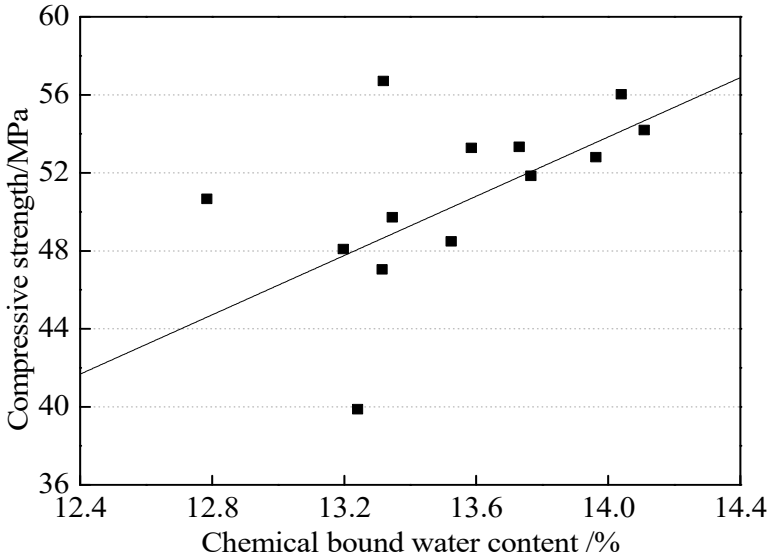

Figure 14. Relationship between compressive strength and chemical binding water content.

3.5.3. Effect of NAC on the Porosity of Hardened Cement

Voids in the section of the NAC cement specimen are shown in Figure 15, and the addition of NAC reducing the porosity of the cement paste is presented in Figure 16.

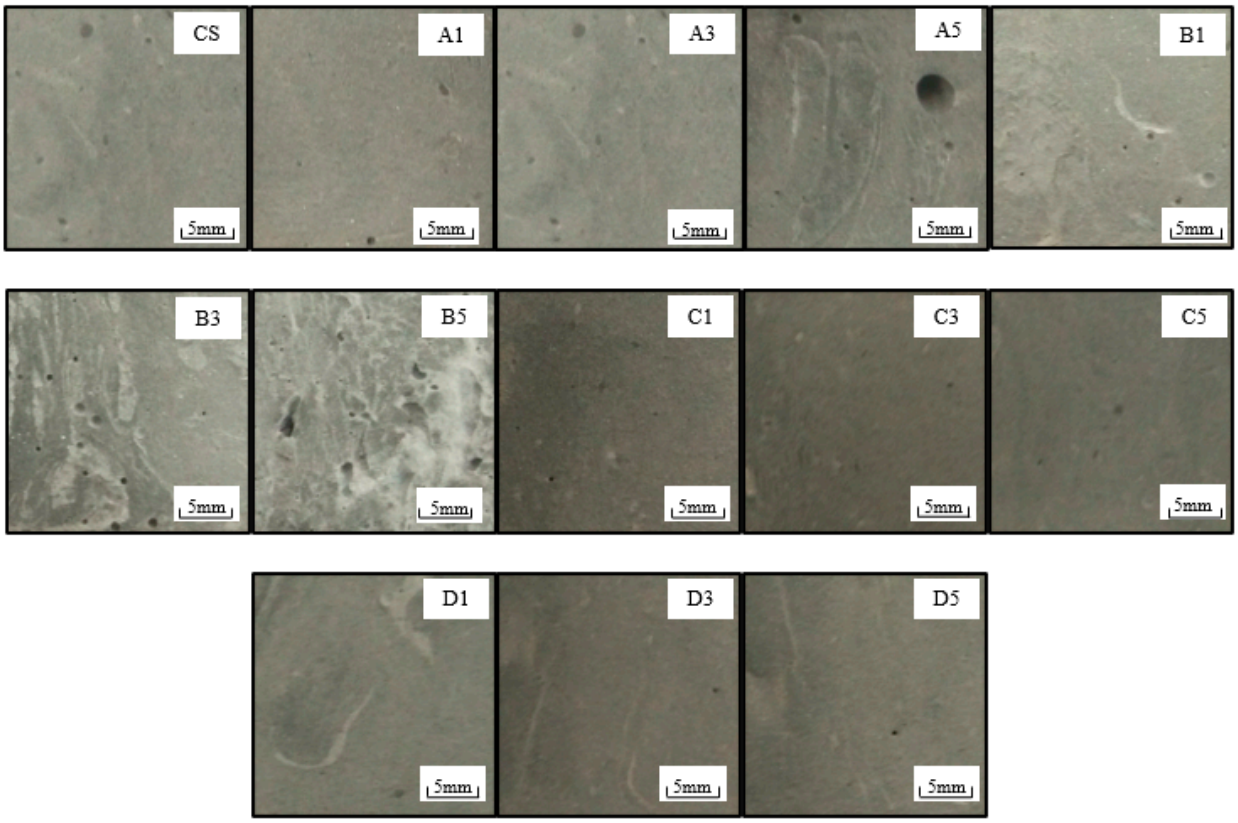

Figure 15. Voids of cement paste section with the calcined NAC.

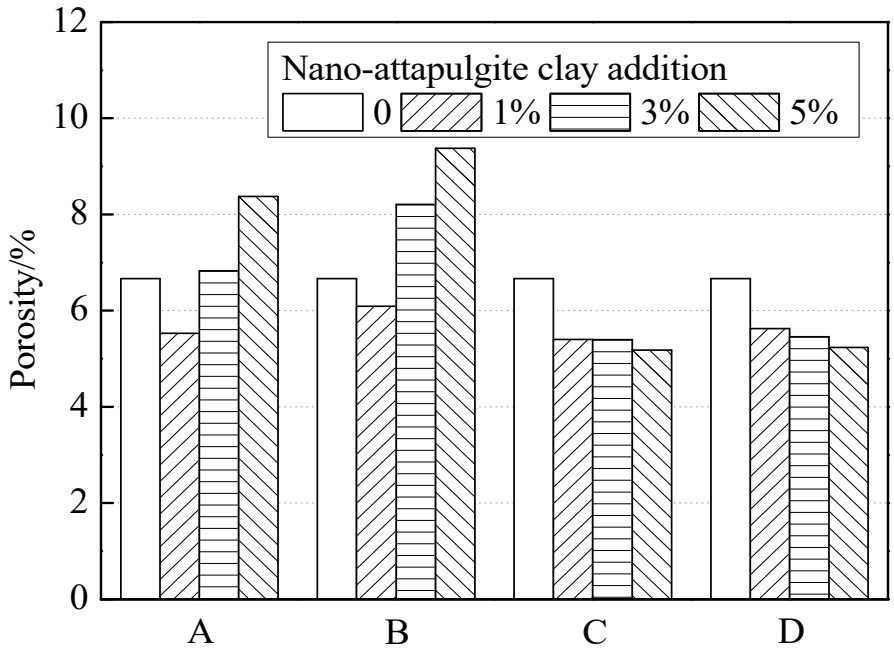

Figure 16. Stomatal content of cement paste with various NAC addition.

From Figure 15, it can be observed that the visible pores of the cement paste mixed with calcined NAC were notably fewer than those of the cement paste mixed with uncalcined NAC and those of the cement paste without NAC. There was a notable number of visible pores in the fracture section of the cement paste mixed with uncalcined NAC raw ore, and the number and the diameter of the pores grew as the mixing amount increased; when the mixing amount reached 5%, visible pores with a diameter of approximately 4 mm appeared. A large number of visible pores emerged in the fracture section of the cement paste mixed with uncalcined NAC high-viscosity ore at a mixing amount of 3%, and the pore diameter stood at around 1 mm. The mixing amount reached 5%, and there were massive irregular pores in the fracture section of the cement paste. The content of visible pores in the fracture section of the cement paste that prominently improved by adding the calcined NAC was remarkably reduced, with only a few pores observable by the naked eye. We can draw that the calcined NAC has the potential to enhance the compactness of the cement paste.

From Figure 16, it can be drawn that adding 3% and 5% uncalculated NAC can reduce the compactness of hardened cement paste and increase the porosity. The porosity of cement mixed with 3% and 5% uncalculated NAC raw ore is 2.44% and 25.58% higher than that of the cement without NAC. The porosity of cement mixed with 3% and 5% uncalculated NAC high-viscosity mineral is 23.07% and 40.62% higher than that of the cement without NAC. This indicated that an uncalculated high-viscosity mineral is not conducive to forming dense hardened cement. Adding calcined NAC can effectively reduce the porosity of hardened cement and improve the compactness, which is consistent with the conclusion in Figure 15. The porosity of hardened cement with 1%, 3%, and 5% NACis 19%, 19.04%, and 22.27% lower than that of the cement without NAC. When the content of NAC with high viscosity is 1%, 3%, and 5%, the porosity of hardened cement paste is 15.58%, 18.1%, and 21.46% lower than that of the cement without NAC, which indicates that calcined NAC raw ore has the best effect in improving the compactness of hardened cement paste. The effect is the best when the content is 5%.

4. Conclusions

This paper mainly studies the improvement of NAC in the hydration process, pore characteristics, and mechanical properties of cement paste under different activation methods. The main conclusions are drawn as follows:

(1) The curing age was 14 days, and the pH value of the pore solution of the cement mixed with the NAC raw ore was 3.96%, 3.95%, and 0.1% lower than that of the cement without NAC. The pH value of the solution in the cement mixed with 5% NAC (calcined) was higher than that of the cement without NAC. When the curing age was14 days, the pH value of the pore solution of the NAC raw ore (calcined) cement was 3.96% higher than that of the cement without NAC, and the pH value of the pore solution of the NAC high-viscosity ore (calcined) cement was 8.8% higher than that of the cement without NAC.

(2) When the mixing amount of uncalcined raw ore and high-viscosity ore was at 5%, the fluidity of the cement was reduced by 45.23% and 57.27%, respectively. The fluidity of the cement mortar mixed with calcined high-viscosity ore (D and E) at a mixing amount of 5% was reduced by 32.66% and 26.13%, respectively, compared to the ordinary specimens.

(3) With the increase in the content, the uncalcined NAC reduces the hydration process of the cement; the chemically bound water content in the raw ore cement with the addition of 3% NAC was 12.78% at 28 days, and the chemical-bound water content in the high-viscosity ore cement was 13.31%. This indicates that the long-term activity of the raw ore is lower than that of the high-viscosity ore. The chemically bound water contents in the 1% and 3% NAC raw (calcined) cement were 14.11% and 14.04%; when the content of calcined NAC raw ore is 1%, the improvement effect on the cement hydration process is the best.

(4) The flexural strength of the cement paste mixed with calcined raw ore and high-viscosity ore at a mixing amount of 1% was generally improved by 28.40% and 17.28%, respectively, when compared to that of the cement without NAC paste. The compressive strength of calcined raw ore cement with a 1%, 3%, and 5% content was 4.5%, 8.06%, and 9.38% higher than cement without NAC. After calcination, the NAC raw ore is better than the high clay ore in improving the mechanical properties of cement.

(5) Adding calcined NAC can effectively reduce the porosity of hardened cement and improve compactness. The porosity of hardened cement with 1%, 3%, and 5% NAC paste was 19%, 19.04%, and 22.27% lower than that of the cement without NAC.

Author Contributions: Writing—original draft, funding acquisition, writing—review and editing, S.Z.; resources, formal analysis, and investigation, Y.F.; methodology, S.P.S. All authors have read and agreed to the published version of the manuscript.

Funding: This research was financially supported by the National Natural Science Foundation of China (Grant No. 51908342), and by the Natural Science Foundation of Shandong Province (Grant No. ZR2018PEE021), to which the authors are very grateful.

Data Availability Statement: Not applicable.

Conflicts of Interest: The authors declare no conflict of interest.

References

1. Suad, A.B.; Emmanuel, K.A. Investigation of corrosion damage in a reinforced concrete structure in Kuwait. *ACI Mater. J.* **1998**, *95*, 226–231.
2. Mahsa, S.; Lars, W. Moisture diffusion coefficients of mortars in absorption and desorption. *Cem. Concr. Res.* **2016**, *83*, 179–187.
3. Da, B.; Yu, H.; Ma, H.; Tan, Y.; Mi, R.; Dou, X. Chloride diffusion study of coral concrete in a marine environment. *Constr. Build. Mater.* **2016**, *23*, 47–58. [CrossRef]
4. Joshani, M.; Koloor, S.S.R.; Abdullah, R. Damage mechanics model for fracture process of steel-concrete composite slabs. *Appl. Mech. Mater.* **2012**, *165*, 339–345. [CrossRef]
5. Naveen, J. Mechanical, fracture, and microstructural assessment of carbon-fiber-reinforced geopolymer composites containing Na_2O. *Polymers* **2021**, *13*, 3852.
6. Mahendran, S. Durability of concrete incorporating fly ash (F-type), rise husk ash and egg shell powder (esp). *Int. J. Earth Sci. Eng.* **2014**, *7*, 1840–1848.
7. Behfarnia, K.; Salemi, N. The effects of nano-silica and nano-alumina on frost resistance of normal concrete. *Constr. Build. Mater.* **2013**, *48*, 580–584. [CrossRef]
8. Aly, M.; Hashmi, M.; Olabi, A.; Messeiry, M.; Abadir, E.; Hussain, A. Effect of colloidal nano-silica on the mechanical and physical behaviour of waste-glass cement mortar. *Mater. Design* **2012**, *33*, 127–135. [CrossRef]
9. Kong, D.; Corr, D.; Hou, P.; Yang, Y.; Shah, S.P. Influence of colloidal silica sol on fresh properties of cement paste as compared to nano-silica powder with agglomerates in micron-scale. *Cem. Concr. Comp.* **2013**, *63*, 30–41. [CrossRef]

10. Hou, P.K.; Cheng, X.; Qian, J.S.; Zhang, R.; Cao, W.; Shah, S.P. Characteristics of surface-treatment of nano-SiO_2 on the transport properties of hardened cement pastes with different water-to-cementratios. *Cem. Concr. Comp.* **2014**, *55*, 26–33. [CrossRef]
11. Cwirzen, A.; Habermehl, C.K. The effect of carbon nano and microfibers on strength and residual cumulative strain of mortars subjected to freeze-thaw cycles. *J. Adv. Concr. Technol.* **2013**, *11*, 80–88. [CrossRef]
12. Frank, C.; John, L.; Wen, H.D. The influences of admixtures on the dispersion, workability, and strength of carbon nanotube-OPC paste mixtures. *J. Cem. Concr. Comp.* **2012**, *34*, 201–207.
13. Schmidt, M.; Amrhein, K.; Braun, T.; Glotzbach, C.; Kamaruddin, S.; Tänzer, R. Nanotechnological improvement of structural materials—Impact on material performance and structural design. *J. Cem. Concr. Comp.* **2013**, *36*, 3–7. [CrossRef]
14. Ramezanianpour, A.A.; Jovein, H.B. Influence of metakaolin as supplementary cementing material on strength and durability of concretes. *Constr. Build. Mater.* **2012**, *30*, 470–479. [CrossRef]
15. Mahdi, V.; Farhad, P.; Mohammad, S.; Khani, S. Comparing a natural pozzolan, zeolite, to metakaolin and silica fume in terms of their effect on the durability characteristics of concrete: A laboratory study. *Constr. Build. Mater.* **2013**, *41*, 879–888.
16. Ern, R. Microstructure formation of cement mortars modified by superabsorbent polymers. *Polymers* **2021**, *13*, 3584.
17. Fereshteh, A.S.; Nicolas, A.L.; Mohammad, S. Mechanical and durability properties of self consolidating high performance concrete incorporating natural zeolite, silica fume and fly ash. *Constr. Build. Mater.* **2013**, *44*, 175–184.
18. Chai, M.; Zhang, H.; Zhang, J.; Zhang, Z. Effect of cement additives on unconfined compressive strength of warm and ice-rich frozen soil. *Constr. Build. Mater.* **2017**, *149*, 861–868. [CrossRef]
19. Yuan, Q.; Zhou, D.; Li, B.; Huang, H.; Shi, C. Effect of mineral admixtures on the structural build-up of cement paste. *Constr. Build. Mater.* **2018**, *160*, 117–126. [CrossRef]
20. Qian, Y.; de Schutter, G. Enhancing thixotropy of fresh cement pastes with nanoclay in presence of polycarboxylate ether superplasticizer (PCE). *Cem. Concr. Res.* **2018**, *111*, 15–22. [CrossRef]
21. Varela, H.; Barluenga, G.; Palomar, I. Influence of nanoclays on flowability and rheology of SCC pastes. *Constr. Build. Mater.* **2020**, *243*, 118285. [CrossRef]
22. Kawashima, S.; Chaouche, M.; Corr, D.J.; Shah, S.P. Rate of thixotropic rebuilding of cement pastes modified with highly purified attapulgite clays. *Cem. Concr. Res.* **2013**, *53*, 112–118. [CrossRef]
23. Zhang, S.; Fan, Y.; Jia, Z.; Ren, J. Effect of nano-kaolinite clay on rebar corrosion and bond behavior between rebar and concrete. *J. Mater. Civil Eng.* **2021**, *33*, 04020416. [CrossRef]
24. Saba, A.M.; Khan, A.H.; Akhtar, M.N.; Khan, N.A.; Koloor, S.S.R.; Petrů, M.; Radwan, N. Strength and flexural behavior of steel fiber and silica fume incorporated self-compacting concrete. *J. Mater. Res. Technol.* **2021**, *12*, 1380–1390. [CrossRef]
25. Kawashima, S.; Chaouche, M.; Corr, D.J.; Shah, S.P. Influence of purified attapulgite clays on the adhesive properties of cement pastes as measured by the tack test. *J. Cem. Concr. Comp.* **2014**, *48*, 35–41. [CrossRef]
26. Lindgreen, H.; Geike, M.; Kryer, H. Microstructure engineering of Portland cement pastes and mortars through addition of ultrafine layer silicates. *Cem. Concr. Comp.* **2008**, *30*, 686–699. [CrossRef]
27. Qian, Y.; Kawashima, S. Flow onset of fresh mortars in rheometers: Contribution ofpaste deflocculation and sand particle migration. *Cem. Concr. Res.* **2016**, *90*, 97–103. [CrossRef]
28. Wang, Y.Q.; Pan, G.H.; Zhang, J.Y. Research on Application of Attapulgite in Building Material. *Bull. Chin. Ceram. Soc.* **2010**, *29*, 1353–1357.
29. Zhou, Y.; He, X.C.; Wang, Y.G. Effect of tween-80 and SDBS on dispersion stabilization of TiO_2powders in water. *J. Electr. Power Sci. Technol.* **2002**, *17*, 72–75.
30. Zhang, S.; Fan, Y.; Huang, J.; Shah, S.P. Effect of nano-metakaolinite clay on the performance of cement-based materials at early curing age. *Constr. Build. Mater.* **2021**, *291*, 123107. [CrossRef]
31. Fan, Y.; Zhang, S.; Kawashim, S.; Surendra, P.S. Influence of kaolinite clay on the chloride diffusion property of cement-based. *Cem. Concr. Comp.* **2014**, *45*, 117–124. [CrossRef]
32. Chen, T.; Wang, J.; Qing, C.; Peng, S.; Song, Y.; Guo, Y. Effect of heat treatment on structure, morphology and surface properties of palygorskite. *J. Chin. Ceram. Soc.* **2006**, *34*, 1406–1410.